miR-146a–Mediated Extracellular Matrix Protein Production in Chronic Diabetes Complications

Biao Feng,[1] Shali Chen,[1] Kara McArthur,[1] Yuexiu Wu,[1] Subhrojit Sen,[1] Qingming Ding,[2] Ross D. Feldman,[2] and Subrata Chakrabarti[1]

OBJECTIVE—microRNAs (miRNAs), through transcriptional regulation, modulate several cellular processes. In diabetes, increased extracellular matrix protein fibronectin (FN) production is known to occur through histone acetylator p300. Here, we investigated the role of miR-146a, an FN-targeting miRNA, on FN production in diabetes and its relationship with p300.

RESEARCH DESIGN AND METHODS—miR-146a expressions were measured in endothelial cells from large vessels and retinal microvessels in various glucose levels. FN messenger RNA expression and protein levels with or without miR-146a mimic or antagomir transfection were examined. A luciferase assay was performed to detect miR-146a's binding to FN 3′–untranslated region (UTR). Likewise, retinas from type 1 diabetic rats were studied with or without an intravitreal injection of miR-146a mimic. In situ hybridization was used to localize retinal miR-146a. Cardiac and renal tissues were analyzed from type 1 and type 2 diabetic animals.

RESULTS—A total of 25 mmol/L glucose decreased miR-146a expression and increased FN expression compared with 5 mmol/L glucose in both cell types. miR-146a mimic transfection prevented such change, whereas miR-146a antagomir transfection in the cells in 5 mmol/L glucose caused FN upregulation. A luciferase assay confirmed miR-146a's binding to FN 3′-UTR. miR-146a was localized in the retinal endothelial cells and was decreased in diabetes. Intravitreal miR-146a mimic injection restored retinal miR-146a and decreased FN in diabetes. Additional experiments showed that p300 regulates miR-146a. Similar changes were seen in the retinas, kidneys, and hearts in type 1 and type 2 diabetic animals.

CONCLUSIONS—These studies showed a novel, glucose-induced molecular mechanism in which miR-146a participates in the transcriptional circuitry regulating extracellular matrix protein production in diabetes. ***Diabetes*** **60:2975–2984, 2011**

In response to metabolic alterations in hyperglycemia, the activation of several transcription factors and gene expression occurs in the endothelial cells, leading to their structural and functional deficits (1–3). Such changes have been demonstrated in the tissues affected by chronic diabetes complications, including retinal, renal, and cardiac and the heart (2). Increased production of extracellular matrix (ECM) proteins, such as fibronectin (FN), is a characteristic feature of all chronic diabetes complications. FN transcripts are upregulated as a result of abnormal signaling mechanisms in hyperglycemia (1–5).

We and others have demonstrated glucose-induced increased FN synthesis in endothelial cells as well as diabetes-induced augmented FN production in the retina, kidney, and heart (3–5). FN, a glycoprotein of 250 KD, is a key component of the ECM and plays an important role in various cellular events (6,7). Alternative splicing processes FN messenger RNA (mRNA), encoded by a single gene with 50 exons (6,7). In endothelial cells, diabetes-induced upregulation of FN is dependent on endothelin-1 and transforming growth factor-β (8). We have additionally shown that transcription coactivator p300 regulates FN upregulation in endothelial cells and in several organs involved in chronic diabetes complications (e.g., retina and heart) (3,9,10).

Hyperglycemia-induced oxidant injury damages DNA, causing activation of several nuclear proteins and subsequent activation of transcription factors and gene expression (1,3,11). Gene transcription, however, depends on transcriptional coactivators and other epigenetic changes at the nuclear levels, including histone acetylation, deacetylation, DNA methylation, phosphorylation, and microRNA (miRNA) alteration (12,13). We have previously demonstrated that glucose-induced activation of transcription factor p300 is a key mechanism in the upregulation of multiple transcription factors and ECM proteins (10).

miRNAs are endogenous regulators produced as small, nonprotein coding RNAs (12–14). Mature miRNA sequences are single stranded, ~19–24 nucleotides in length, and are highly conserved among species. They mostly act to negatively regulate gene expression at the posttranscriptional level, by interacting with their target mRNA 3′–untranslated region (UTR) (14,15). Most target mRNA predictions for miRNAs stem from computational analyses examining sequence complementarity. In mammals, it is estimated that over one-third of genes are regulated by miRNAs. On average, one miRNA may regulate 100–200 different target genes, and a single gene may have several target sites for various miRNA (15,16). miRNAs are important players in a variety of cellular processes (12,15). Upregulation of miR-320 has been demonstrated in the cardiac microvascular endothelial cells in type 2 diabetic rats (17,18). We and others have demonstrated alterations of miR-133a in cardiomyocyte hypertrophy in diabetes and in other cardiomyopathies (19–21). We recently have demonstrated that miR-200b downregulation plays a pathogenetic role in increased permeability and angiogenesis through vascular endothelial growth factor (VEGF) in diabetic retinopathy (22). However, to date there are no studies showing a link between miRNA alteration and early changes, such as increased ECM protein production in diabetes. Furthermore,

From the [1]Department of Pathology, Schulich School of Medicine and Dentistry and the University of Western Ontario, London, Ontario, Canada; and the [2]Department of Medicine, Schulich School of Medicine and Dentistry and the University of Western Ontario, London, Ontario, Canada.

Corresponding author: Subrata Chakrabarti, subrata.chakrabarti@schulich.uwo.ca.

Received 8 April 2011 and accepted 22 July 2011.

DOI: 10.2337/db11-0478

This article contains Supplementary Data online at http://diabetes.diabetesjournals.org/lookup/suppl/doi:10.2337/db11-0478/-/DC1.

it is not clear whether such miRNA-mediated gene regulation in diabetes interacts with other epigenetic changes regulating ECM protein expression, such as histone acetylation.

miR-146a has been shown to be an important regulator of the innate immune response (23) and plays an important role in several inflammatory processes (24–27). Oxidative stress and inflammatory processes have been demonstrated to be important contributors in the pathogenesis of several chronic diabetes complications (28–31). Furthermore, as a result of such inflammatory processes, increased ECM protein production, a characteristic pathologic component of chronic diabetes complications, occurs in several diabetes complications, including diabetic retinopathy and nephropathy (29–31). ECM protein FN, which is characteristically upregulated in all chronic diabetes complications, is a target of miR-146a (www.targetscan.org and www.microrna.org). Hence, we investigated whether miR-146a alteration occurs in chronic diabetes complications and if such alterations play any role in FN production.

Because endothelial cells are a major target of glucose-mediated damage in chronic diabetes complications and in tissues like retina, they are a main source of increased FN production in diabetes. We investigated endothelial cells from large vessels and from the retina to characterize glucose-induced miR-146a–mediated regulation of FN production. We expanded our study to investigate the retina of diabetic animals. We further examined kidneys and hearts, from both type 1 and type 2 diabetic animals, for similar abnormalities.

RESEARCH DESIGN AND METHODS

Cell culture. Human umbilical-vein endothelial cells (HUVECs) were obtained from Clonetics and were cultured as previously described (3). Appropriate concentrations of glucose were added to the medium. L-Glucose was used as a control. All experiments were carried out after 24 h of incubation, unless otherwise indicated. Three different batches of cells, each in duplicate, were investigated. Bovine retinal microvascular endothelial cells (BRMECs) were obtained from VEC Technologies (Rensselaer, NY) and were grown in a defined endothelial cell growth medium (MCDB-131 complete). We have previously described the culture conditions (22). Twenty-four hours before transfection, the cells were passaged in the six-well plate (Corning, Acton, MA) coated with FN (Sigma). Human embryonic kidney (HEK) 293A cells were obtained from the American Type Culture Collection and were used as previously described by us and others (22,32). Cell viability was examined by a trypan blue dye exclusion test and was expressed as a percentage of the trypan blue–negative cells in controls (1,33). All experiments were performed at least in triplicate. All reagents were obtained from Sigma Chemicals (Sigma, Oakville, ON, Canada), unless otherwise specified.

miRNA mimic or antagomir transfection. The HUVECs and BRMECs were transfected with miRIDIAN miRNA-146a mimic or antagomir (20 nmol/L) (Dharmacon, Chicago, IL) using the transfection reagent Lipofectamine2000 (Invitrogen, ON, Canada). miRIDIAN miRNA mimic or antagomir or scrambled control were used in parallel. miRNA transfection efficiency was determined by real-time RT-PCR.

Generation of adenoviral p300 short-hairpin RNA. Adenoviral constructs were generated with an AdMax adenovirus vector creation kit, as per the manufacturer's instructions (Microbix BioSystems, Toronto, ON, Canada). In brief, shuttle vector pDC312U6 was constructed by inserting the U6 promoter PCR fragment into the Xba I and *Bam*H I sites of pDC312. Short-hairpin RNA (shRNA) sequences, specific for p300 (A: TTCGCCGCAGCGGACCGGC; B: GCGGCCTAAACTCTCATCT; and C: TCAGCTTCAGACAAGTCTT), were ligated into pDC312U6 by *Bam*H I and *Eco*R I sites. Resultant recombinant shuttle plasmids were cotransfected into HEK293A cells along with genomic plasmid. Virus was harvested 2 weeks after transfection and amplified in HEK293A cells (34).

Animal experiments. The animal experiments were performed in accordance with regulations specified by the Canadian Council on Animal Care. The University of Western Ontario Animal Care and Veterinary Services approved all protocols. This investigation conforms to the *Guide for the Care and Use of Laboratory Animals* published by the National Institutes of Health (NIH publ. no. 85-23, revised 1996).

Male SD rats, weighing 150–200 g, were obtained (Charles River, Saint-Constant, Canada). Diabetes was induced by a single intraperitoneal injection of streptozotocin (STZ) (65 mg/kg, in citrate buffer). Age- and sex-matched rats were used as controls and given equal volumes of citrate buffer. Diabetes was defined as a blood glucose level >20 mmol/L on 2 consecutive days (Abbott Diabetes Care, Alameda, CA). The animals were fed on a standard rodent diet and water ad libitum. Some diabetic animals received weekly intravitreal injections of 1.5 μg miR-146a mimic or antagomir in lipofectamine reagent in one eye, whereas the other eye received scrambled control, for 4 weeks (22). Likewise, groups of diabetic animals also received weekly intravitreal injections of 1.5 μg p300 small-interfering RNA (siRNA) in one eye and scrambled control siRNA in the other eye, as previously described (10). The animals were killed 1 week after the fourth injection, and the retinal tissues were collected and stored at −70°C. Renal cortical tissues and left ventricular myometrium also were similarly collected and stored.

To investigate the role of miR-146a in type 2 diabetes, male *db/db* mice and controls were purchased from the Jackson Laboratories. After the onset of diabetes, they were monitored regularly. After 2 months of follow-up, the animals were killed and the retinal, renal, and cardiac tissues were collected.

miRNA extraction and analysis. miRNAs were extracted from the cells and tissues using the mirVana miRNA isolation kit (Ambion, Austin, TX). In brief, the cells were collected and washed two times using PBS. The tissues were homogenized in lysis/binding solution. miRNA additive (1:10) was added to the samples on ice for 15 min. Equal volumes of acid-phenol:chloroform were added to the cell suspension and the tissue lysate and mixed for 30 s by vortex. After centrifugation and removal of the aqueous phase, the mixture was added 1.25-fold to 100% ethanol. The mixture was passed through the filter cartridge and eluted with elution solution. Real-time PCR was used with a final reaction volume of 20 μL containing 10 μL TaqMan 2 × Universal PCR Master Mix (No AmpErase UNG), 8 μL nuclease-free water, 1 μL TaqMan microRNA assay (Applied Biosystems, Carlsbad, CA), and 1 μL RT product. The data were normalized to RNU6B small nuclear RNA to account for differences in reverse-transcription efficiencies and the amount of template in the reaction mixtures.

mRNA extraction and RT-PCR. RNA was extracted with TRIzol reagent (Invitrogen Canada, Burlington, ON, Canada), as previously described (1,3,10). Total RNA (2 μg) was used for cDNA synthesis by using a high-capacity cDNA reverse-transcription kit (Applied Biosystems). Real-time quantitative RT-PCR was performed using the LightCycler (Roche Diagnostics Canada, Laval, QC, Canada). Melting-curve analysis was used to determine the melting temperature (T_m) of specific amplification products and primer dimers. For each gene, the specific T_m values were used for the signal acquisition step (2–3°C below T_m). The data of FN and p300 RT-PCR were normalized to β-actin or 18S mRNA to account for differences in reverse-transcription efficiencies and the amount of template in the reaction mixtures. The methodologies and the primers were used as previously described (3,10).

Protein extraction and enzyme-linked immunosorbent assay for FN. The cells were collected after transfection for 24 h and lysed by a radioimmunoprecipitation assay buffer. Tissues were homogenized by adding the radioimmunoprecipitation buffer. The proteins were collected and the concentrations tested using a bicinchoninic acid kit (Thermo Fisher Scientific, Rockford, IL). ELISA for FN was performed using commercially available kits for human FN (Millipore, Billerica, MA) and rat FN (Kamiya Biomedical, Seattle, WA), according to the manufacturers' instructions. Western blot for acetylated H3 lysine was performed, as previously described, using acetylated H3 lysine antibody (Abcam, Cambridge, MA) (3). The signals were detected using horseradish peroxidase–conjugated secondary antibody (Santa Cruz Biotechnology) and developed using the chemiluminescent substrate (Amersham Pharmacia Biotechnology, Amersham, U.K.).

Luciferase reporter assay for targeting FN 3′-UTR. For luciferase reporter experiments, a human FN 3′-UTR segment of 617 bp and a rat FN 3′-UTR segment of 644 bp were amplified by PCR from human and rat cDNA and inserted into the pMIR-REPORT luciferase vector with cytomegalovirus promoter (Applied Biosystems) using the Sac I and Hind III sites immediately downstream from the stop codon of luciferase. The following sets of primers were used to generate specific fragments: for human FN 3′-UTR, forward primer 5′-AGAGCTC ATCATCTTTCCAATCCAGAGGAAC-3′ and reverse primer 5′-TCAAGCTT TAATCACCCACCATAATTATACC-3′; and for rat FN 3′-UTR, forward primer 5′-AGAGCTC TCCAGCCCAAGCCAACAAGTG-3′ and reverse primer 5′-TCAAGCTT TCCACAGTAGTAAAGTGTTGGC-3′ (underlined sequences indicate the endonuclease restriction site). Nucleotide substitutions were introduced by PCR mutagenesis to yield mutated binding site. The primers for human and rat FN 3′-UTR mutation cloning are listed in Supplementary Table 1. The DNA sequence of the cloned product was confirmed by sequencing. The pMIR–FN 3′-UTR, miR-146a mimic, and pMIR-REPORT β-galactosidase control plasmid were then cotransfected into HEK293A cells for 24 h. After transfection, luciferase activity was measured using the Dual-Light Chemiluminescent Reporter Gene Assay System (Applied Biosystems), following the manufacturer's instructions.

Luciferase activity was read using the Chemiluminescent SpectraMax M5 (Molecular Devices, Sunnyvale, CA) (22,32). Luciferase activity was normalized for transfection efficiency by measuring β-galactosidase activity, according to the manufacturer's instructions. The experiments were performed in triplicate.

Immunohistochemistry. Rat retinal sections were immunocytochemically stained for FN using anti-FN antibody (1:100; Dako Canada, Burlington, ON, Canada). These methods have been previously described (22). No antibody- and isotype-matched IgG controls were used.

In situ hybridization. Five-micrometer-thick retinal tissue sections from paraffin-embedded blocks were transferred to positively charged slides. 5′ and 3′ double DIG–labeled custom-made mercury locked nucleic acid (LNA) miRNA detection probes (Exiqon, Vedbaek, Denmark) were used to detect miR-146a expression using an in situ hybridization (ISH) kit (Biochain Institute, Hayward, CA), as described (22,32). Scrambled probes and no-probe controls were used as controls.

Statistical analysis. Data are expressed as means ± SEM, and the statistical significance of the results were analyzed by ANOVA and the Student t test, as appropriate. A $P < 0.05$ was considered significant.

RESULTS

Glucose causes downregulation of miR-146a in the endothelial cells. Based on the hypothesis that glucose-induced augmented FN production may, in part, be regulated by miR-146a, we investigated HUVECs exposed to 5 and 25 mmol/L glucose for 24 h. These concentrations are based on our previous dose-dependent analysis of FN mRNA and protein expression (1,5,8). We confirmed the upregulation of FN mRNA and protein following incubation with 25 mmol/L D-glucose but not by 25 mmol/L L-glucose (osmotic control) (Fig. 1*A*). We then extracted miRNA from these cells. Quantitative RT-PCR analysis of the endothelial cells in 25 mmol/L glucose confirmed significant downregulation of miR-146a compared with 5 mmol/L glucose. No effects were seen after incubation with 25 mmol/L L-glucose (Fig. 1*B*).

Glucose-induced FN upregulation in endothelial cells is mediated by miR-146a. We then proceeded to explore functional significance of miR-146a downregulation with respect to FN expression, which is a target for miR-146a. Glucose-induced miR-146a downregulation was associated with increased FN mRNA production, as detected by real-time PCR (Fig. 1*A* and *B*). Simultaneously, FN protein levels also were increased after incubation with 25 mmol/L glucose (Fig. 1*C*). To find a cause-and-effect relationship, we transfected cells in 25 mmol/L glucose with miR-146a mimics. Transfection efficiencies, assessed by measuring miR-146a expression, showed almost a sixfold increase in intracellular miR-146a expression compared with scrambled miRNA transfection (Fig. 1*B*).

miR-146a mimic transfection reduced basal FN expression. Such transfection also normalized glucose-induced FN upregulation, indicating that glucose-induced FN upregulation is mediated through miR-146a. No such effects were seen in scrambled mimics (Fig. 1*A* and *C*). On the other hand, transfection of the endothelial cells in 5 mmol/L glucose with miR-146a antagomirs produced a glucose-like effect, leading to augmented FN mRNA production (Fig. 1*A*). In parallel, ELISA analyses showed that glucose-induced increased FN protein production in the endothelial cells can be prevented by miR-146a mimic transfection (Fig. 1*C*).

To further establish a direct relevance of our findings in the context of diabetic retinopathy, we examined whether similar changes occur in the retinal microvascular endothelial cells. Our results show that 25 mmol/L glucose (compared with 5 mmol/L glucose) caused a significant downregulation of miR-146a (Fig. 1*D*) in BRMECs. In parallel, FN mRNA was upregulated after exposure to 25 mmol/L glucose. Transfection of miR-146a mimics lead to an almost 15-fold increase in intracellular miR-146a. miR-146a mimic transfection reduced basal FN expression and prevented glucose-induced FN upregulation. Furthermore, similar to HUVECs, transfection of the BRMECs with miR-146a antagomirs produced a glucose-like upregulation of FN (Fig. 1*E*).

miR-146a binds to the 3′-UTR of the FN gene. We then wanted to confirm that the effects of miR-146a are indeed mediated by direct binding of miR-146a with the 3′-UTR of the FN gene. To do this, we carried out luciferase assays. Such assays were performed in HEK293A cells. Luciferase reporter plasmids were prepared, containing cloned miR-146a binding sites for the FN 3′-UTR (of both rat and human FN in separate experiments) or mutated 3′-UTR. The plasmids were cotransfected with miR-146a mimic, causing overexpression of miR-146a. Such miR-146a overexpression significantly repressed FN 3′-UTR luciferase activity. However, no such repression was seen when we performed similar experiments using mutated 3′-UTR (Fig. 2). These data indicated that binding of miR-146a with the 3′-UTR of the FN gene was required to produce its effects.

miR-146a is present in the retina and is downregulated in diabetes. After establishing that miR-146a regulated FN in HUVECs and in BRMECs, we expanded our study to investigate whether the mechanisms seen in these cells were important in the development of retinal microangiopathy in a well-established animal model. STZ-induced diabetic rats showed hyperglycemia (serum glucose of diabetes 23.5 ± 3.7 mmol/L vs. controls 5.3 ± 0.4 mmol/L, $P < 0.001$) and reduced body weight (body weight of diabetes 304.2 ± 58.8 g vs. controls 400.7 ± 32.4 g, $P < 0.001$). We initially performed real-time PCR analysis of the retinal tissue from rats after 1 month of diabetes. We selected this time point because we have previously shown that diabetes-induced increased ECM protein and vasoactive factor expression is established at this time point (2,3). Real-time PCR analysis demonstrated that 1 month of poorly controlled diabetes causes significant downregulation of miR-146a (Fig. 3*A*). We further confirmed these results using in situ hybridization and LNA probes. miR-146a was localized in the neuronal, glial, and endothelial cells in the retina. Overall expression was reduced in the retina in diabetes, including that in the endothelial cells (Fig. 3*B*).

Diabetes-induced FN upregulation in the retina is mediated by miR-146a. To establish the functional consequence of miR-146a downregulation in the retina, we investigated retinal FN mRNA and protein expression, which is a target for miR-146a. Diabetes-induced miR-146a downregulation was associated with FN mRNA upregulation, as detected by real-time PCR (Fig. 3*C*). Simultaneously, FN protein levels also were increased in the retina in diabetic rats (Fig. 3*D*). To find a cause-and-effect relationship, we performed intravitreal miR-146a mimic injection. Intraretinal delivery efficiencies, assessed by measuring miR-146a expression in the retina, showed an almost 60-fold increase in retinal miR-146a expression (Fig. 3*E*). Such intravitreal miR-146a injection normalized diabetes-induced FN upregulation. No such repression was seen after the injection of scrambled mimics (Fig. 3*C* and *D*). We also carried out immunocytochemical analyses, which showed positivity for FN, particularly around microvessels, as previously described (35). Such expressions were pronounced in diabetes and were reduced after the intravitreal mimic injection (Supplementary Fig. 1).

Glucose-induced miR-146a downregulation is mediated through transcriptional coactivator p300 in the endothelial cells and in the retina. We previously have demonstrated that p300-mediated histone acetylation is

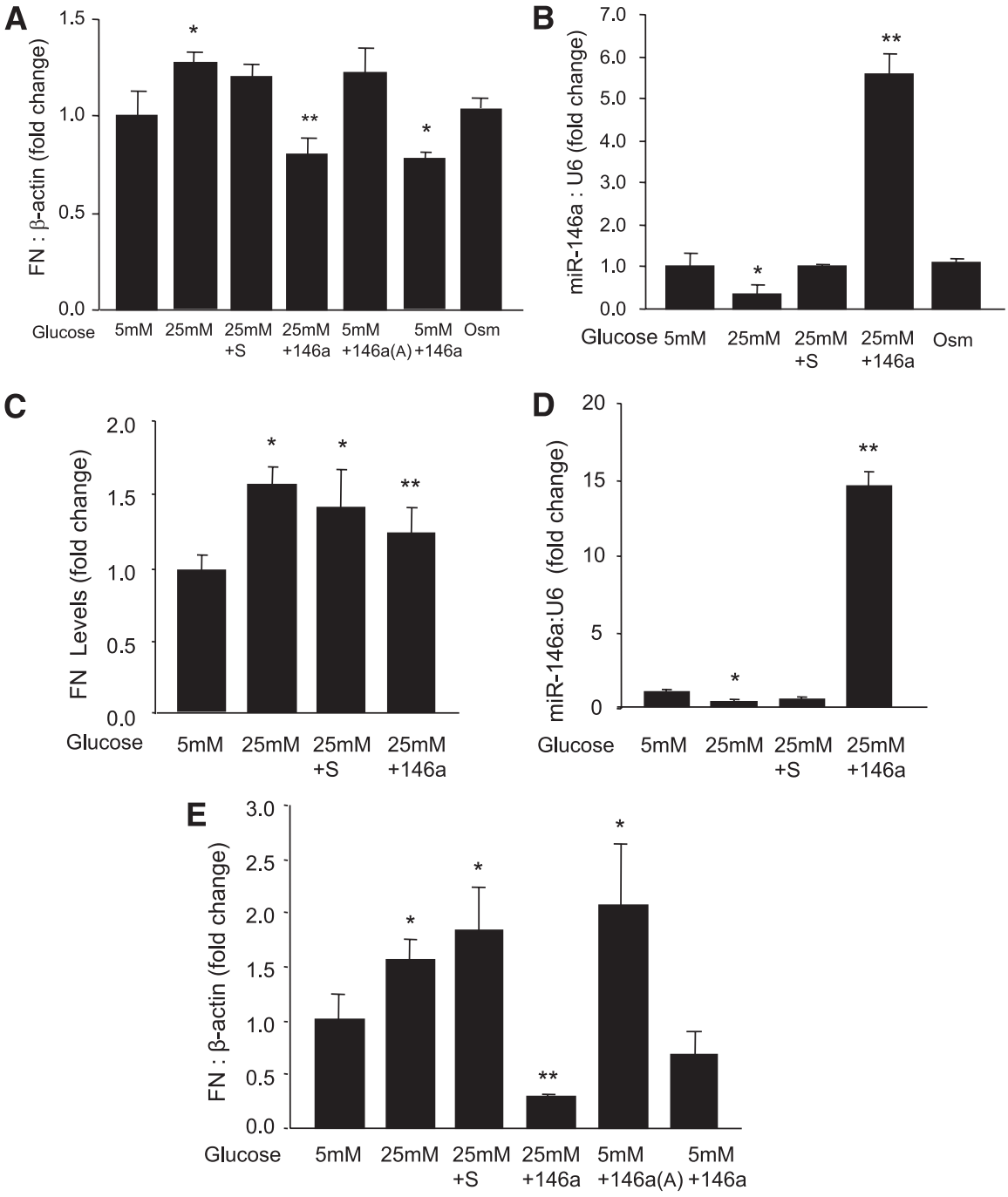

FIG. 1. Endothelial cells (HUVECs) exposed to 25 mmol/L (25 mM) glucose (compared with 5 mmol/L [5 mM] glucose) showed increased FN mRNA (*A*) and reduced miR-146a expression (*B*). Such changes were not seen when the cells were incubated with 25 mmol/L L-glucose (osmotic control [Osm]). Transfection of endothelial cells with miR-146a mimics (but not the scrambled mimics) reduced basal FN expression and normalized glucose-induced upregulation of FN mRNA (*A*) and FN protein (*C*). *A*: The glucose-like effect (FN upregulation) was further seen when cells in 5 mmol/L glucose were transfected with miR-146a antagomir. *B*: The efficiency of miR-146a mimic transfection by increased miR-146a expression following miR-146a mimic transfection compared with scrambled mimics. Likewise, BRMECs showed glucose-induced miR-146a downregulation (*D*) and FN upregulation (*E*). *E*: Transfection of BRMECs with miR-146a mimics reduced basal FN expression and also normalized HG-induced upregulation of FN mRNA. *D*: The efficiency of miR-146a mimic transfection by increased miR-146a expression following miR-146a mimic transfection compared with scrambled mimics. 146a, miR-146a mimic; 146a(A), miR-146a antagomir; S, scrambled miRNA. *Significantly different from 5 mmol/L glucose; **significantly different from 25 mmol/L glucose, miRNA levels are expressed as a ratio of RNU6B (U6); mRNA levels are expressed as a ratio to β-actin and normalized to 5 mmol/L glucose.

a key event causing transcription of multiple proteins, including FN, in response to hyperglycemia in the endothelial cells (3,10). Furthermore, epigenetic phenomena, such as acetylation, are thought to play a significant role in the regulation of miRNA production (12). Hence, we explored the relationship of p300 in this scenario. In keeping with our previous data, in endothelial cells 25 mmol/L glucose caused significant upregulation of p300 mRNA and acetylation of histone proteins (Fig. 4*A* and *B*). Transfection of p300 shRNA significantly prevented miR-146a downregulation and FN overexpression (Fig. 4*C* and *D*). Likewise, we examined retinal tissues from diabetic and age- and

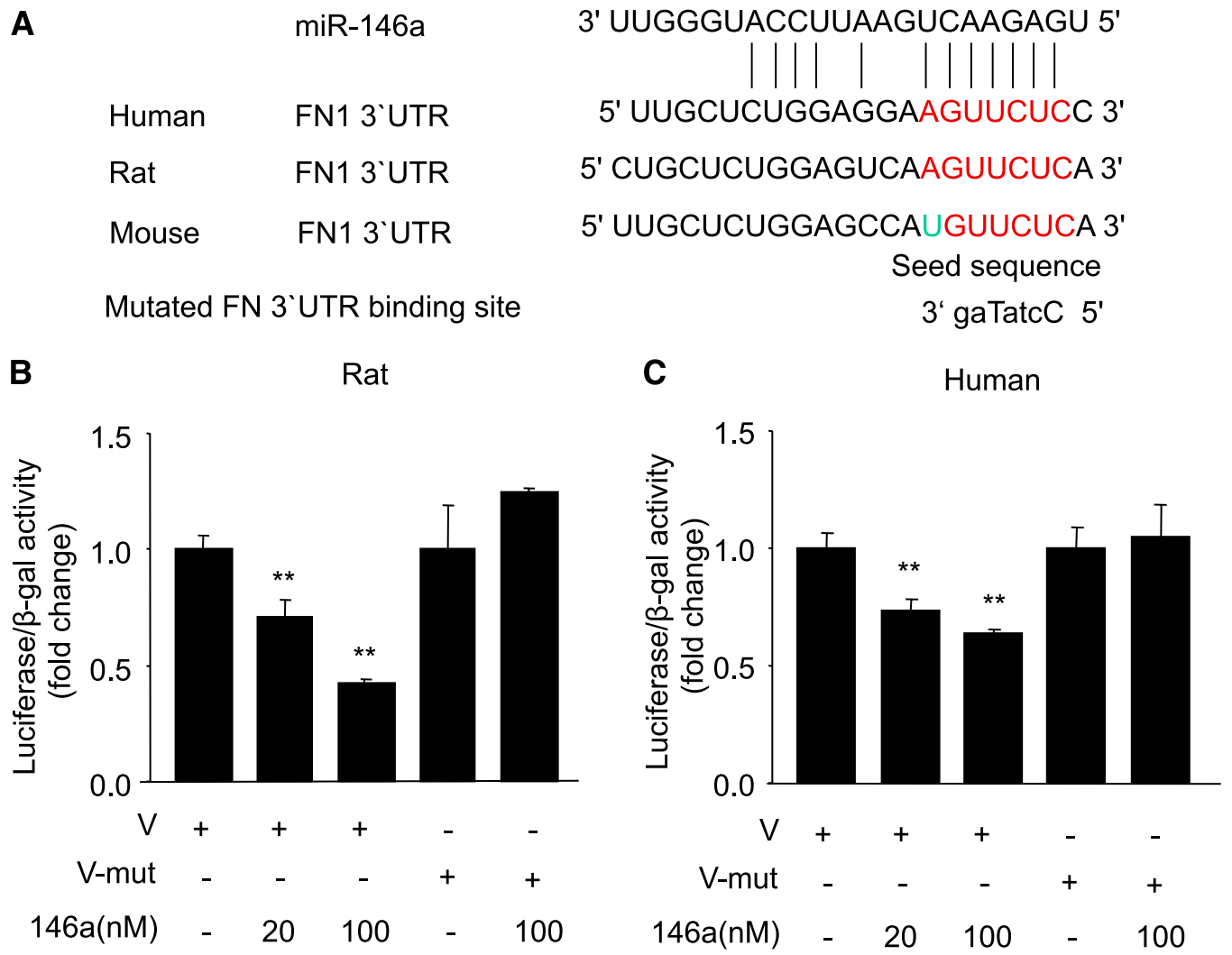

FIG. 2. *A*: **Alignment of FN 3′-UTR (and mutated FN 3′-UTR) sequence with mature miR-146a based on bioinformatics predictions (www.targetscan.org, www.microrna.org, and www.ebi.ac.uk1). The 5′ end of the mature miR-146a is the seed sequence and has perfect complementarity with seven nucleotides of the 3′-UTR of FN. In the mutated sequence (small caps identifying mutated nucleotides), such complementarity was lost.** *B* **and** *C*: **Luciferase reporter assay using rat and human FN, respectively, showing dose-dependent binding of FN 3′-UTR with miR-146a, whereas mutated (mut) FN 3′-UTR abrogated the inhibitory effects of miR-146a. Relative luciferase activities were expressed as luminescence units and normalized for β-galactosidase expression. **Significantly different from vector (V) or mut V, FN 3′-UTR luciferase plasmids plus β-galactosidase plasmids; V-mut, mutated FN 3′-UTR luciferase plasmids plus β-galactosidase plasmids. (A high-quality color representation of this figure is available in the online issue.)**

sex-matched control rats. Diabetes caused increased retinal FN and p300 mRNA expression. Intravitreal p300 siRNA injection led to reduced p300 mRNA and restoration of miR-146a levels, reduction of diabetes-induced increased FN expression (Fig. 4*E*–*G*). On the other hand, miR-146a mimic transfection did not prevent glucose-induced p300 overexpression (Fig. 4*H*).

Reduced miR-146a in association with augmented p300 and FN expression is present in several organs in type 1 and type 2 diabetes. We then asked the question whether the changes we saw are retina specific or are present in other organs, such as kidney and heart, which also are affected by chronic diabetes complications. To this extent, we investigated FN and p300 mRNA expression analysis and performed miR-146a analyses from the cardiac and renal tissues of STZ-induced diabetic rats. Poorly controlled diabetes for 1 month cause augmented FN and p300 mRNA expression in association with reduced miR-146a levels in the kidney and heart (Fig. 5*A*–*F*). To further examine whether such changes occur also in type 2 diabetes, we examined retinal, renal, and cardiac tissues from *db/db* mice after 2 months of poorly controlled diabetes. At this time point, these animals developed several changes characteristic of chronic diabetes complications (20,28). *Db/db* mice demonstrated hyperglycemia (serum glucose; diabetes 29.1 ± 2.5 mmol/L and controls 8.9 ± 2.7 mmol/L, $P < 0.05$) and increased body weight (diabetes 44.4 ± 2.5 g and controls 34 ± 2.5 g, $P < 0.05$) compared with controls. Similar to the type 1 diabetes model, diabetic *db/db* mice showed augmented FN and p300 mRNA expression in the retina, kidney, and heart in association with reduced miR-146a levels (Fig. 6*A*–*I*).

DISCUSSION

In this study, we have shown that glucose-induced FN upregulation in endothelial cells and in the retina of diabetic rats is mediated through miR-146a. Using miR-146a

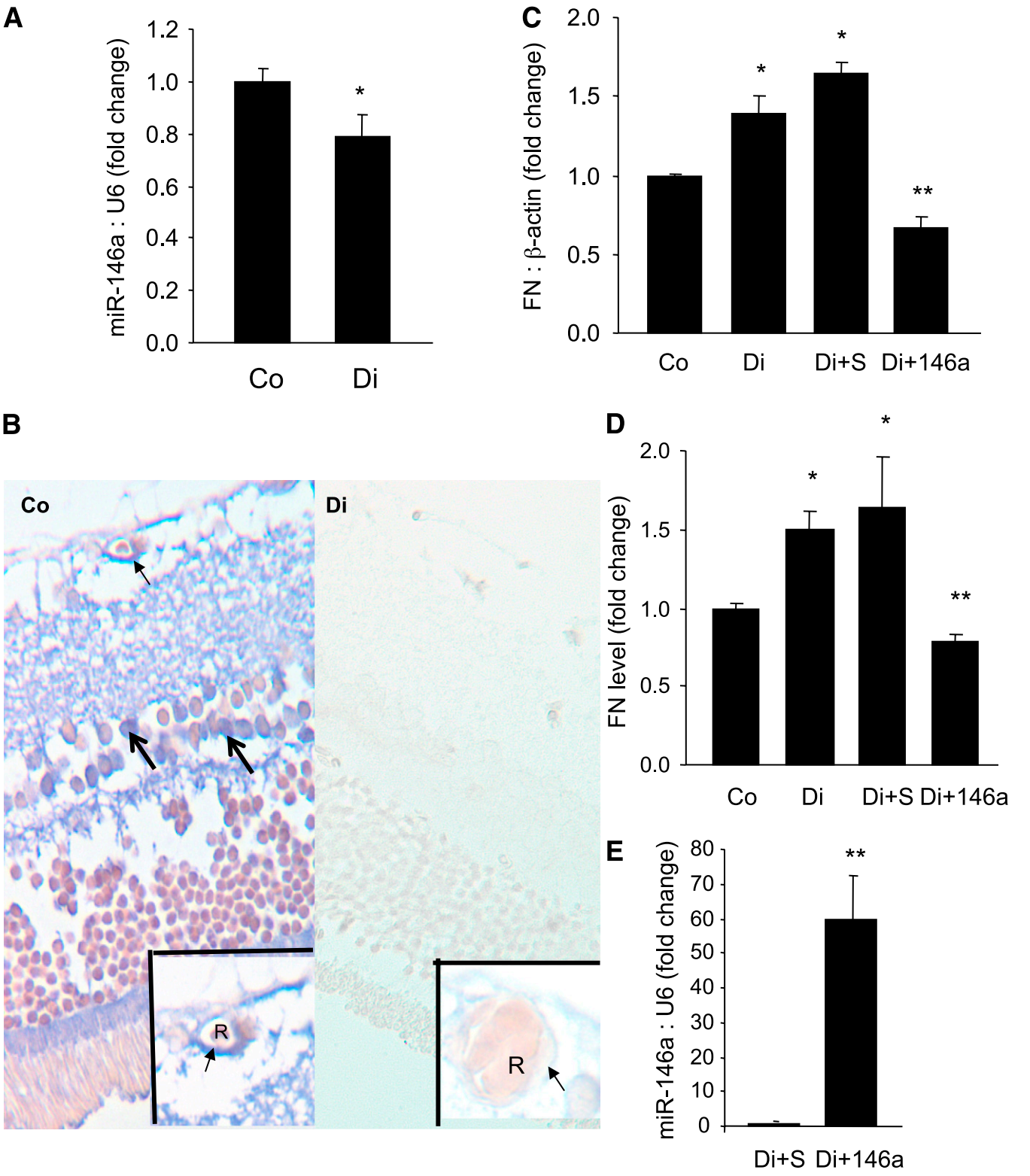

FIG. 3. miR-146a–mediated alteration of retinal FN. *A*: Poorly controlled diabetes caused a reduction of rat retinal miR-146a levels. *B* and *C*: Representative LNA-ISH study of retinal tissues in a control (Co) and a diabetic (Di) rat retina showing localization of miR-146a (blue chromogen) in the retinal capillaries (arrow) and in the cells of inner nuclear layer (large arrow), possibly both in the glial and neuronal elements. *Insets* show an enlarged view of the capillary with miR-146a localization (arrow) in a control rat and reduced level of endothelial miR-146a in the retina of a diabetic rat (arrow). Diabetes-induced augmented FN mRNA (*C*) and protein levels (*D*) (as measured by ELISA) in the rat retina can be prevented by intravitreal miR-146a mimic (but not by scrambled [S] mimics) injection. *E*: Efficiency of intravitreal delivery as demonstrated by increased retinal miR-146a expression after an intravitreal injection of miR-146a mimic compared with scrambled mimic. *Significantly different from control; **significantly different from diabetic or diabetic plus scrambled. miRNA levels are expressed as a ratio of RNU6B (U6) normalized to control or diabetic plus scrambled (*E*). mRNA levels are expressed as a ratio to β-actin and normalized to control. Alkaline phosphatase was used as chromogen (blue) with no counterstain in LNA-ISH. R, red blood cell. (A high-quality digital representation of this figure is available in the online issue.)

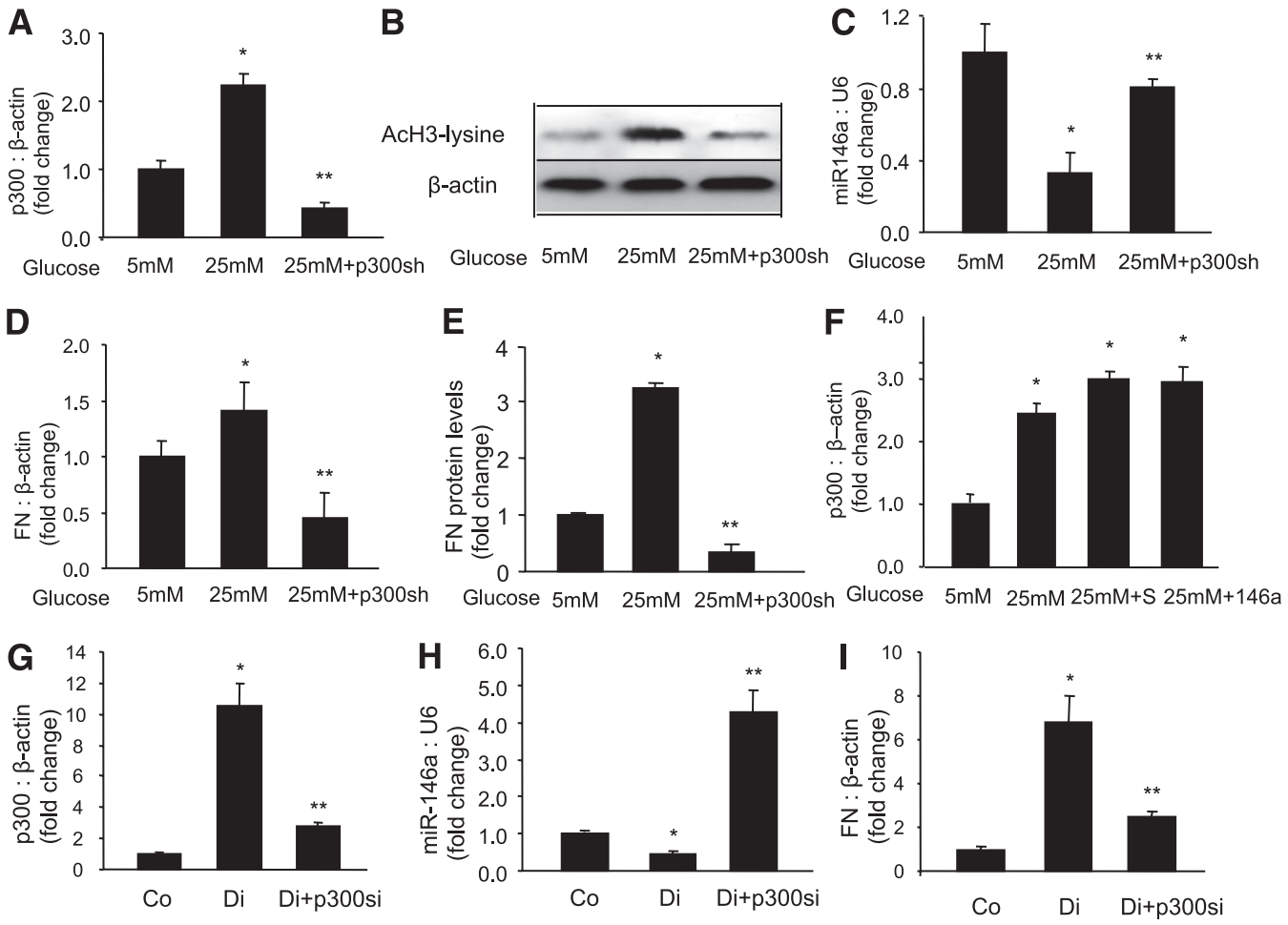

FIG. 4. miR-146a levels are regulated with p300. In the endothelial cells, 25 mmol/L (25 mM) glucose-induced p300 mRNA upregulation (*A*) and increased histone acetylation (*B*) were prevented by p300 shRNA (p300sh) transfection. In the endothelial cells, p300 shRNA also prevented glucose-induced reduced miR-146a production (*C*) and FN mRNA (*D*) and FN protein upregulation (*E*) in the HUVECs. In parallel, diabetes-induced retinal p300 upregulation (*G*), miR-146a downregulation (*H*), and FN upregulation (*I*) were prevented by intravitreal p300 siRNA (p300si) injection. *F*: No significant differences were seen with respect to p300 mRNA expression when cells in 25 mmol/L glucose were transfected with miR-146a mimic or scrambled (S) mimic. *Significantly different from 5 mmol/L glucose or control (Co); **significantly different from 25 mmol/L glucose or diabetes (Di). miRNA levels are expressed as a ratio of RNU6B (U6); mRNA levels are expressed as a ratio to β-actin normalized to control or 5 mmol/L (5 mM) glucose.

mimic transfection, we also have directly demonstrated that diabetes-induced FN upregulation can be blocked by increasing the availability of miR-146a and that hyperglycemia further regulates this process through transcription coactivator p300. We have further showed that such a process is prevalent in the retina, kidney, and heart in both type 1 and type 2 diabetes.

In diabetes, overproduction of superoxides by the mitochondrial electron transport chain as a result of hyperglycemia increases proton gradient and causes DNA damage and activation of several nuclear proteins leading to the activation of transcription factors and gene expression (11). miRNAs provide another level of transcriptional regulation. miRNAs, by binding with the 3′-UTR of the specific mRNA, causes their degradation or translational repression (12,13, 15,16). Several lines of evidence have recently been presented to demonstrate that miRNAs play a significant role in a large number of, if not all, cellular process (12,13, 15,16). In mammals, it is estimated that over one-third of genes are regulated by miRNAs. Here, we describe the role of miR-146a in causing FN overexpression in diabetes. We initially demonstrated miR-146a downregulation in glucose-exposed cells. We showed, using the luciferase assay, that miR-146a binds with rat and human FN gene 3′-UTR. Then, we directly demonstrated the functional significance of miR-146a downregulation with respect to FN expression and the relationship with p300. We further showed that this mechanism is of functional significance in an animal model of diabetic retinal microangiopathy.

One of the major glucose-induced dysfunctions includes augmented ECM protein production. Increased ECM is deposited in the tissue, which manifests as structural changes, such as basement-membrane thickening, focal scarring, mesangial matrix expansion, etc. (1–4,11). We and others have demonstrated glucose-induced increased collagen 1α (IV) and FN synthesis in the endothelial cells and in retina, kidney, and heart in diabetes (1–4). FN plays an important role in various cellular events (6–8). We also have demonstrated that glucose-induced FN upregulation is mediated through p300-dependent histone acetylation (3). In our study, we characterized another level of regulation of glucose-induced FN gene expression through specific miRNAs. We have shown that p300 regulates miR-146a–mediated FN upregulation, further establishing that

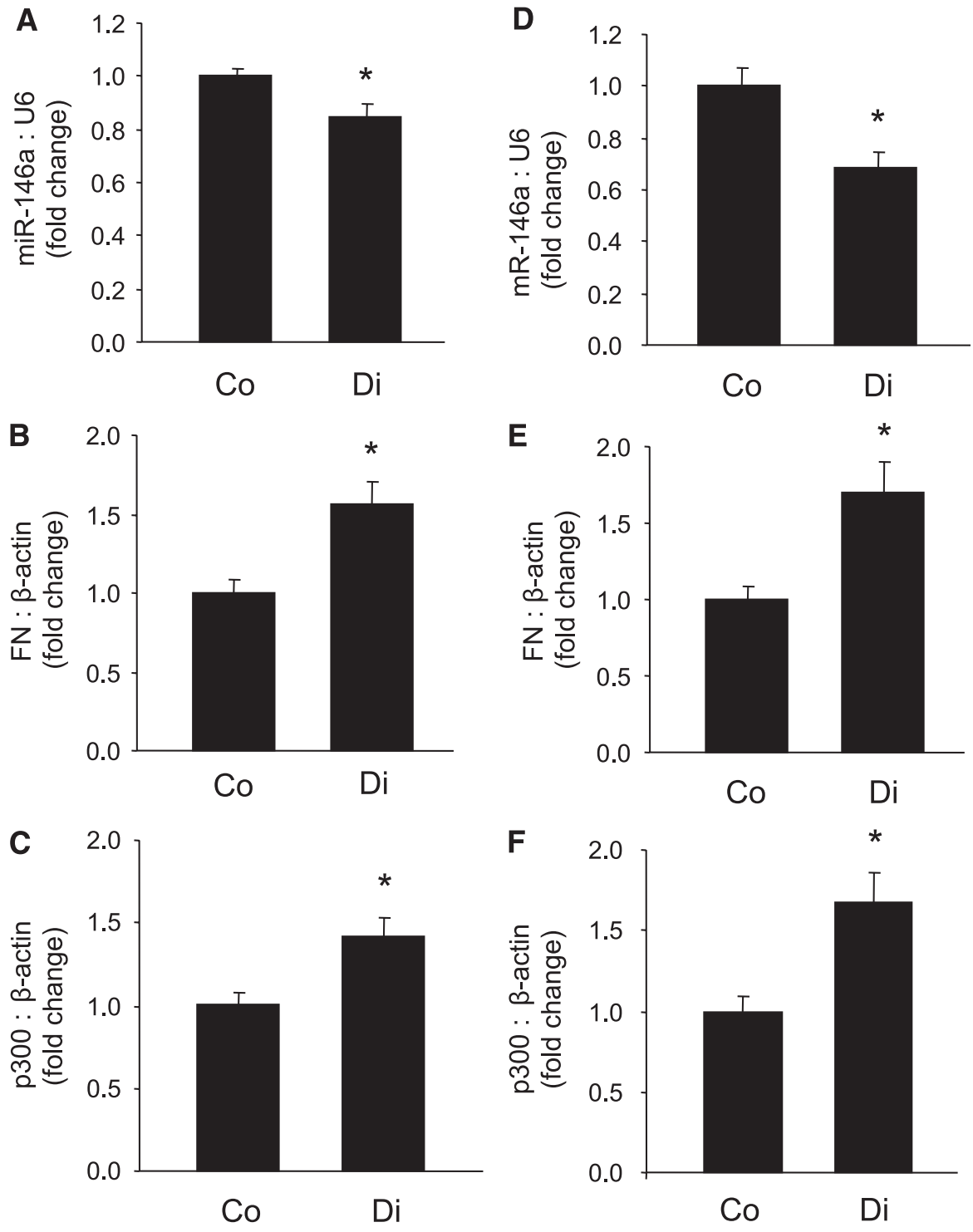

FIG. 5. In the heart (*left column*) and kidneys (*right column*) of type 1 diabetic (STZ induced) rats, miR-146a levels were reduced (*A* and *D*) and FN mRNA (*B* and *E*) and p300 mRNA (*C* and *F*) levels were elevated after 1 month of poorly controlled diabetes (Di). *Significantly different from control (Co), miRNA levels are expressed as a ratio of RNU6B (U6) normalized to control; mRNA levels are expressed as a ratio to β-actin normalized to control.

such epigenetic mechanisms of tissue damage are important in chronic diabetes complications.

There are no previous studies in the literature with respect to miRNA and FN alteration in diabetic retinal microangiopathy. Among other miRNAs, miR-377 and miR-192 have been shown to be involved in diabetic nephropathy (36–38). Hearts from diabetic rabbits demonstrated reduced miR-133a modulating HERG K^+ channel causing QT prolongation (39). We have demonstrated the down-regulation of miR-133a in cardiomyocyte hypertrophy in diabetes (20). We also have recently demonstrated that miR-200b plays an important role in diabetic retinopathy through VEGF modulation. Of interest, miR-200b modulates p300 expression (22).

Although there are no previous works characterizing the role of miR-146a in retinopathy or in other diabetes

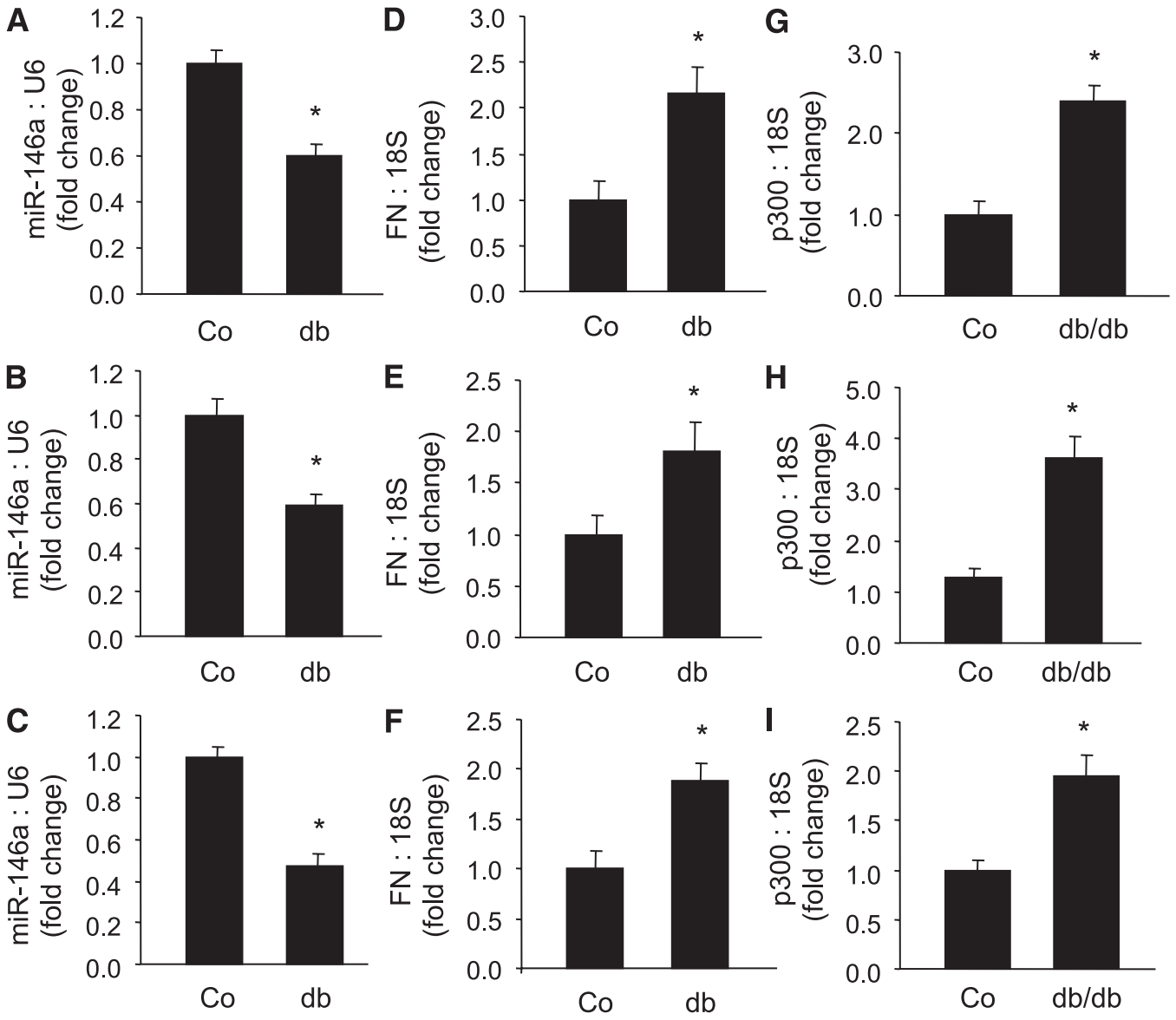

FIG. 6. In the retina (*upper row*), heart (*middle row*), and kidneys (*lower row*) of type 2 diabetic (*db/db*) mice, miR-146a levels were reduced (*A–C*) and FN mRNA (*D–F*) and p300 mRNA (*G–I*) levels were elevated after 2 months of poorly controlled diabetes (db). *Significantly different from control (Co), miRNA levels are expressed as a ratio of RNU6B (U6) normalized to control; mRNA levels are expressed as a ratio to β-actin normalized to control.

complications, miR-146a downregulation has been demonstrated to play a key role in innate immunity, inflammatory responses, viral infections, and in some malignancies (25–27). We have previously demonstrated that p300 siRNA transfection in endothelial cells and in the retina causes significant reduction in the activities of several transcription factors and generation of downstream vasoactive factors and ECM proteins (3,10). In keeping with this notion, this study has demonstrated that miR-146a is regulated by transcription coactivator p300. We have previously demonstrated that several vasoactive factors also are regulated through p300 (3,10). Hence, it is possible that through mir-146a, p300 regulates several such transcripts of interest. A detailed analysis of such processes needs additional specific experiments. On the other hand, it is also probable that p300 regulates gene expression independent of miR-146a. In keeping with such notion, we have shown that p300 regulates VEGF expression, which is not a target of miR-146a (3). Hence, regulatory mechanisms with regard to specific factors and other ECM proteins, not investigated in this manuscript, may be different and need additional specific investigations. The current study further provides a link among miR-200b, miR-146a, and p300, where miR-200b regulates p300 expression, which in turn regulates miR-146a expression and controls FN expression. It is of further interest to note that it is possible that miR-146a may influence several other inflammatory cytokines, which are of importance in the context of retinopathy and other chronic diabetes complications (27–30). In addition, other miRNAs also may regulate FN expression. A related microRNA (i.e., miR-146b) is, however, located in a different chromosome and possibly does not have any direct regulatory effects on FN (www.targetscan.org and www.microrna.org). The specific role of miR-146a in such processes has to be established in the future through specific experiments.

miRNAs are important for both physiological and pathological conditions. They have been implicated as players in a variety of cellular processes, such as differentiation, proliferation, apoptosis, metabolism, and in feedback loops for various signal transduction pathways (12,15). Because miRNAs are such important players in normal physiological processes, their dysregulation or abnormal expression could lead to a variety of diseases. Hence, they potentially can be used as drugs. Our study shows that miR-146a treatment prevents increased ECM protein production, a characteristic feature of chronic diabetes complications. Development of therapies using an RNA-based approach is advantageous because of its specificity compared with a protein/receptor targeting approach. However, from a mechanistic standpoint, one miRNA regulates multiple genes, and one gene potentially may be regulated by multiple miRNAs. Hence, targeting one or a few miRNAs provides potential unique opportunities to prevent multiple gene expression and for the development of RNA-based therapeutics.

ACKNOWLEDGMENTS

This work was supported by grants from the Canadian Diabetes Association (to S.Cha.) and the Heart and Stroke Foundation of Ontario (to S.Cha. and R.D.F.).

No potential conflicts of interest relevant to this article were reported.

B.F. researched data, contributed to discussion, and reviewed and edited the manuscript. S.Che., K.M., Y.W., S.S., Q.D., and R.D.F. researched data and reviewed and edited the manuscript. S.Cha. researched data, contributed to discussion, and wrote, reviewed, and edited the manuscript.

REFERENCES

1. Chen S, Mukherjee S, Chakraborty C, Chakrabarti S. High glucose-induced, endothelin-dependent fibronectin synthesis is mediated via NF-kappa B and AP-1. Am J Physiol Cell Physiol 2003;284:C263–C272
2. Chen S, Khan ZA, Cukiernik M, Chakrabarti S. Differential activation of NF-kappa B and AP-1 in increased fibronectin synthesis in target organs of diabetic complications. Am J Physiol Endocrinol Metab 2003;284:E1089–E1097
3. Chen S, Feng B, George B, Chakrabarti R, Chen M, Chakrabarti S. Transcriptional coactivator p300 regulates glucose-induced gene expression in endothelial cells. Am J Physiol Endocrinol Metab 2010;298:E127–E137
4. Roy S, Cagliero E, Lorenzi M. Fibronectin overexpression in retinal microvessels of patients with diabetes. Invest Ophthalmol Vis Sci 1996;37:258–266
5. Xin X, Khan ZA, Chen S, Chakrabarti S. Extracellular signal-regulated kinase (ERK) in glucose-induced and endothelin-mediated fibronectin synthesis. Lab Invest 2004;84:1451–1459
6. Astrof S, Hynes RO. Fibronectins in vascular morphogenesis. Angiogenesis 2009;12:165–175
7. Pankov R, Yamada KM. Fibronectin at a glance. J Cell Sci 2002;115:3861–3863
8. Khan ZA, Chan BM, Uniyal S, et al. EDB fibronectin and angiogenesis: a novel mechanistic pathway. Angiogenesis 2005;8:183–196
9. Chiu J, Khan ZA, Farhangkhoee H, Chakrabarti S. Curcumin prevents diabetes-associated abnormalities in the kidneys by inhibiting p300 and nuclear factor-kappaB. Nutrition 2009;25:964–972
10. Kaur H, Chen S, Xin X, Chiu J, Khan ZA, Chakrabarti S. Diabetes-induced extracellular matrix protein expression is mediated by transcription coactivator p300. Diabetes 2006;55:3104–3111
11. Brownlee M. Biochemistry and molecular cell biology of diabetic complications. Nature 2001;414:813–820
12. Chuang JC, Jones PA. Epigenetics and microRNAs. Pediatr Res 2007;61:24R–29R
13. Latronico MV, Catalucci D, Condorelli G. MicroRNA and cardiac pathologies. Physiol Genomics 2008;34:239–242
14. Liu J, Valencia-Sanchez MA, Hannon GJ, Parker R. MicroRNA-dependent localization of targeted mRNAs to mammalian P-bodies. Nat Cell Biol 2005;7:719–723
15. He L, Hannon GJ. MicroRNAs: small RNAs with a big role in gene regulation. Nat Rev Genet 2004;5:522–531
16. Ørom UA, Lund AH. Experimental identification of microRNA targets. Gene 2010;451:1–5
17. Ren XP, Wu J, Wang X, et al. MicroRNA-320 is involved in the regulation of cardiac ischemia/reperfusion injury by targeting heat-shock protein 20. Circulation 2009;119:2357–2366
18. Wang XH, Qian RZ, Zhang W, Chen SF, Jin HM, Hu RM. MicroRNA-320 expression in myocardial microvascular endothelial cells and its relationship with insulin-like growth factor-1 in type 2 diabetic rats. Clin Exp Pharmacol Physiol 2009;36:181–188
19. Dong DL, Chen C, Huo R, et al. Reciprocal repression between microRNA-133 and calcineurin regulates cardiac hypertrophy: a novel mechanism for progressive cardiac hypertrophy. Hypertension 2010;55:946–952
20. Feng B, Chen S, George B, Feng Q, Chakrabarti S. miR133a regulates cardiomyocyte hypertrophy in diabetes. Diabetes Metab Res Rev 2010;26:40–49
21. Carè A, Catalucci D, Felicetti F, et al. MicroRNA-133 controls cardiac hypertrophy. Nat Med 2007;13:613–618
22. McArthur K, Feng B, Wu Y, Chen S, Chakrabarti S. MicroRNA-200b regulates vascular endothelial growth factor–mediated alterations in diabetic retinopathy. Diabetes 2011;60:1314–1323
23. Chassin C, Kocur M, Pott J, et al. miR-146a mediates protective innate immune tolerance in the neonate intestine. Cell Host Microbe 2010;8:358–368
24. Chen T, Li Z, Jing T, et al. MicroRNA-146a regulates the maturation process and pro-inflammatory cytokine secretion by targeting CD40L in oxLDL-stimulated dendritic cells. FEBS Lett 2011;585:567–573
25. Nahid MA, Satoh M, Chan EK. Mechanistic role of microRNA-146a in endotoxin-induced differential cross-regulation of TLR signaling. J Immunol 2011;186:1723–1734
26. Perry MM, Moschos SA, Williams AE, Shepherd NJ, Larner-Svensson HM, Lindsay MA. Rapid changes in microRNA-146a expression negatively regulate the IL-1beta-induced inflammatory response in human lung alveolar epithelial cells. J Immunol 2008;180:5689–5698
27. Li L, Chen XP, Li YJ. MicroRNA-146a and human disease. Scand J Immunol 2010;71:227–231
28. Chiu J, Xu BY, Chen S, Feng B, Chakrabarti S. Oxidative stress-induced, poly(ADP-ribose) polymerase-dependent upregulation of ET-1 expression in chronic diabetic complications. Can J Physiol Pharmacol 2008;86:365–372
29. Lopes de Faria JB, Silva KC, Lopes de Faria JM. The contribution of hypertension to diabetic nephropathy and retinopathy: the role of inflammation and oxidative stress. Hypertens Res 2011;34:413–422
30. Kern TS. Contributions of inflammatory processes to the development of the early stages of diabetic retinopathy. Exp Diabetes Res 2007;2007:95103
31. Joussen AM, Poulaki V, Le ML, et al. A central role for inflammation in the pathogenesis of diabetic retinopathy. FASEB J 2004;18:1450–1452
32. Wang M, Tan LP, Dijkstra MK, et al. miRNA analysis in B-cell chronic lymphocytic leukaemia: proliferation centres characterized by low miR-150 and high BIC/miR-155 expression. J Pathol 2008;215:13–20
33. Chen S, Khan ZA, Karmazyn M, Chakrabarti S. Role of endothelin-1, sodium hydrogen exchanger-1 and mitogen activated protein kinase (MAPK) activation in glucose-induced cardiomyocyte hypertrophy. Diabetes Metab Res Rev 2007;23:356–367
34. Gros R, Van Uum S, Hutchinson-Jaffe A, et al. Increased enzyme activity and beta-adrenergic mediated vasodilation in subjects expressing a single-nucleotide variant of human adenylyl cyclase 6. Arterioscler Thromb Vasc Biol 2007;27:2657–2663
35. Kuiper EJ, Hughes JM, Van Geest RJ, et al. Effect of VEGF-A on expression of profibrotic growth factor and extracellular matrix genes in the retina. Invest Ophthalmol Vis Sci 2007;48:4267–4276
36. Kato M, Zhang J, Wang M, et al. MicroRNA-192 in diabetic kidney glomeruli and its function in TGF-beta-induced collagen expression via inhibition of E-box repressors. Proc Natl Acad Sci USA 2007;104:3432–3437
37. Wang Q, Wang Y, Minto AW, et al. MicroRNA-377 is up-regulated and can lead to increased fibronectin production in diabetic nephropathy. FASEB J 2008;22:4126–4135
38. Villeneuve LM, Natarajan R. The role of epigenetics in the pathology of diabetic complications. Am J Physiol Renal Physiol 2010;299:F14–F25
39. Xiao J, Luo X, Lin H, et al. MicroRNA miR-133 represses HERG K+ channel expression contributing to QT prolongation in diabetic hearts. J Biol Chem 2007;282:12363–12367